Prostate Disease Diagnosis from CT Images Using Multi-Class Support Vector Machine

Wafaa A. Abbas†, Salema S. Salman† and Ban S.Ismael††

† Department of Clinical Laboratory of Sciences, College of Pharmacy, University of Baghdad, Baghdad, Iraq.
††Department of Astronomy and Space of Sciences, College of Science, University of Baghdad, Baghdad, Iraq.

Abstract
Prostate disease is very common now men (adult and advanced in years old), all patients of prostate disease are having similar symptoms, it is difficult to diagnose malignant prostate at an early stage because of the noise corrupts medical images of CT scan. In this study bilateral filtering, Image sharpening and contrast stretching are implemented for medical image denoising,edge enhancement and evaluation of medical image quality respectively, to enhance medical images which correlated with early diagnosis of prostate cancer from CT image using multiclass support vector machine (SVM) classification method. Thirteen features extracted from 20 ×20-pixel block of each slice of CT that the prostate appears in it, which is used later for the training and test SVM approach. xperimental results demonstrate that the SVM approach gives the best performance to the classification between normal and abnormal prostate by 100%, while Multi-SVM is not quite appropriate to identify the prostate cancer where the medical diagnosis using CT scan succeeded by 65% in identifying cancer. rostate size calculated for Iraqi normal adults, by two methods, ellipsoid approach and frustum Approach where the prostate size varies with age, it becomes significantly larger in older men. The prostate gland tends to enlarge, around the age of 40. The two methods gave success in the computation of size using CT image, where they showed a significant match in the results.
Keywords:
Malignant Prostate, CT image, SVM, Diagnosis prostate cancer.

1. Introduction

The prostate is a walnut-shaped male reproductive gland. The job of the prostate is producing and secreting a thin, alkaline fluid that constitutes (20 -30) % of the ejaculate, located between the bladder and the penis[1,2] figure (1). The prostate is just in front of the rectum. The prostate diseases are

1- Inflammation of the prostate, sometimes caused by infection, it is treated with antibiotics.
2- Prostatic hypertrophy or BPH called enlarged prostate, prostate growth affects virtually all men over fifty years, it is treated by Medicines or surgery.
3- Prostate cancer is the most common form of cancer in men. Surgery, radiation, hormone therapy, and chemotherapy can be used for the treatment.

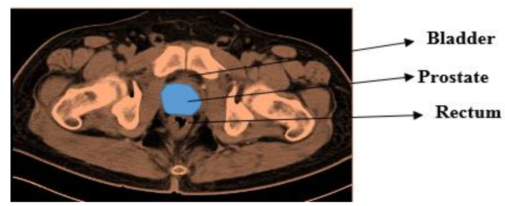

A

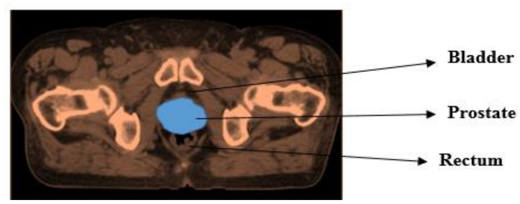

B

Fig. 1 Prostate in Abdomen CT image test (A) Normal (B) Abnormal

The most deduce malignancies in men over the age of sixty years is prostate cancer. Thousands of men die of prostate cancer. Prostate cancer can be treated in its early stages. the methods available for the early stage detection of prostate cancer are Prostate specific Antigen (PSA) screening and Digital Rectal Examination [3]. PSA screening is not completely dependable, since Prostatic hypertrophy and Inflammation of the prostate can also cause an increase in Prostate-specific Antigen. Also, normal Prostate-specific Antigen does not completely rule out prostate. Although Digital Rectal Examination is low cost and a short time to get the results, it discovers tumor when it reaches a volume offensive biological activity [3].
Imaging has now become the dominant trend for Prostate cancer revelation and localization, mostly, imaging techniques such as (MIR) Magnetic Resonance Imaging and (TRUS) Trans Rectal Ultra Sound imaging are proposed only if carcinoma is suspected [4,5]. Magnetic Resonance Imaging, being costly, is done to locate and quantify carcinoma. The Trans Rectal Ultra Sound imaging provides correct diagnosis, it is painful and costly. Currently, CT images are used in cancer therapy for guiding radiotherapy as long as the cancer is in its early stage [6]. Imaging techniques preferable to obtain images of soft

Manuscript received January 5, 2019
Manuscript revised January 20, 2019

tissues behind bone structures are (CT), it is lower cost, short imaging time and common availability. A modern multi-slice CT enables the fast acquirement of careful sets of successive images with a very high resolution supporting a more confident diagnosis. The images have a clear conception of anatomical features and structures.
The texture is characterized by pixel patterns in an area around a pixel. A number of methods statistical have been developed for texture feature extraction, since the advent of researchers in the medical image field. Statistical methods commonly used in medical image analysis are (Contrast, Correlation, Energy, Homogeneity, Entropy, Root mean square, Smoothness, Kurtosis, Skewness). The aim of the Statistical feature extraction is to assist in the diagnosis and clinical studies, it has also shown that Statistical feature extraction provides an effective tool in Medical image classification [7].

2. Materials

The dataset sources in the present study were prostate CT scan images scanned by Siemens device have been supplied by Al-Shaheed Ghazi Hariri Hospital for specialized surgery. The total number of participants in this study was (12 participants 108 images) individuals which were divided into two groups, normal prostate group (43) persons, and abnormal prostate (65) patients. The images collected from abdomen CT test, each of them has 512x512 pixels of size.

3. Methodology and Results

3.1 Pre Processing CT Image

Image preprocessing steps were implemented using MATLAB. The pre-processing stage is required since the images acquired from the scanning would contain not only prostate but also bone, urinary, bladder, and noises. Therefore, noise elimination and image segmentation are important to obtain the desired images.
The pre-processing step of CT image refers to the enhancement of CT image slice intensity and filtering, stretched contrast, noise reduction, sharpening.

3.1.1 Bilateral Filter

A technique to smooth images, however, preserving edges is bilateral filtering. Bilateral filtering is used in the applications of image processing such as image enhancement and reduceing image distortion [8]. Bilateral Filtering is achieved by the combinations of two Gaussian filters [9]. One filter works in the spatial domain and the second filter works in intensity domain. The Bilateral Filtering applies spatially weighted averaging smoothing edges.
Range filtering is defined:

$$h(x) = k_r^{-1}(x) \iint_{\infty}^{-\infty} f(\,\xi)\, s\left(f(\xi), f(x)\right) d\xi$$

Where $s\left(f(\xi), f(x)\right)$ measures the photographic similarity between the pixel at the neighborhood center x and that of nearby point ξ.
Bilateral filter replaces the pixel value at x with an average of similar and nearby pixel values. In smooth regions, pixel values in a small neighborhood are similar to each other, and the bilateral filter acts basically as a standard domain filter, averaging away the small, weakly correlated differences between pixel values caused by noise. Bilateral filtering is a non-iterative method.

3.1.2 Sharpening

Unsharp masking is an image sharpening technique, is used for edge enhancement. This includes isolating the edges of an image and magnifying them and then placing them back in the image. The process of unsharp masking is composed of two branches. The first branch extracts the edge from the input image (operator negative for the input image, to edge extraction in darker areas). In the second branch, we extract the edge in bright areas followed by the extraction of the result [10].In this section, we demonstrate the performance of the proposed method based bilateral filtering like unsharp masking

3.1.3 Contrast Stretching

A contrast stretch improves the brightness differences uniformly across expand the dynamic range of the image according to a mapping function that specifies an output pixel brightness value for each input pixel brightness value. In this study, the first step bilateral filter applied then in the second step unsharp masking filtering is used for the image sharpening, this sharpening is followed by contrast stretching of image. Figure (2) shows the results of pre-processing steps.

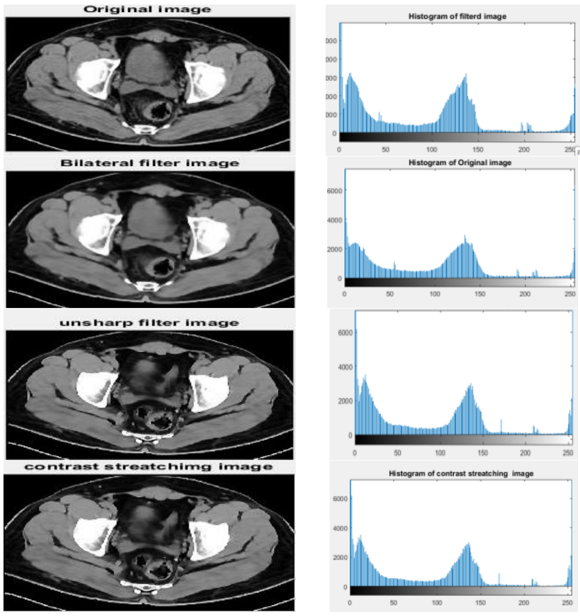

Fig. 2 Pre-processing steps of Abdomen CT image with its histogram.

3.2 Segmentation

In analyzing abdomen CT image, it is important to distinguish the prostate region from its surroundings. We used different segmentation methods to determine the best way for isolating the prostate gland from the surrounding organs, Fuzzy C-mean (FCM) and K-mean methods (unsupervised segmentation) , K-Nearest Neighbor (KNN) and Maximum Likelihood (MLH)) methods (supervised segmentation) are used to separate the prostate region from the abdomen region are usually referred as the segmentation process. The results of the methods shown in figure (3). The algorithms of segmentation are failure to separate the prostate region from the abdomen image due to the overlapping of the organs and the similar density of the surrounding tissues, this makes it hard to isolate prostate from the relevant regions by these methods, So region of Interest (ROI) which identify by the radiologist are used in the next section to separate the prostate region from the abdomen CT image.

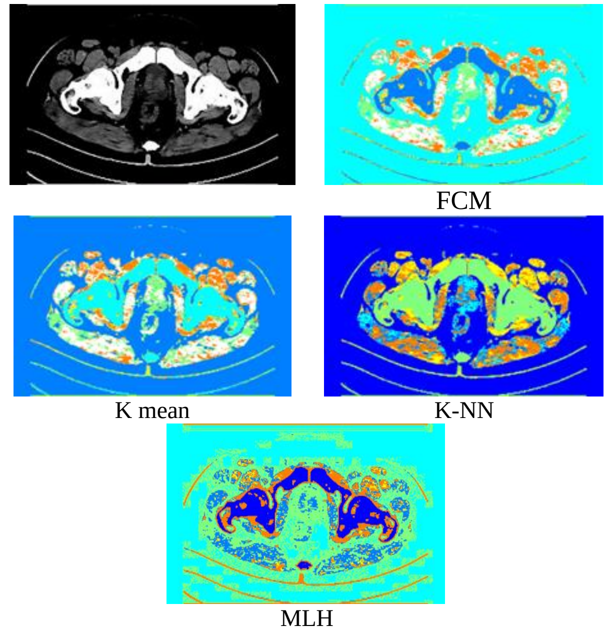

Fig. 3 Segmentation methods to separate prostate from abdomen CT image.

3.2.1The region of Interest (ROI)

The accurate extraction of the ROI is very important because Medical image has rich information and complex structures. The methods used to separate prostate from surrounding are usually referred as a region of interest process. We extracted the prostate region from enhanced abdomen ct image . The ROI from prostate tissue are extracted by selected block of size 20 × 20 Pixels as shown in the figure (4 -A) which used to extract the statistical features of prostate, while all prostate region extracted from the sequence image of each case manually by draw line curve around prostate region using cropping tools in Matlab as shown in figure (4-B) used later to calculate the area of slice, then determine prostate gland size.

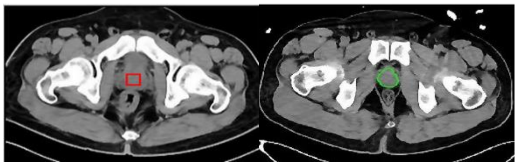

A

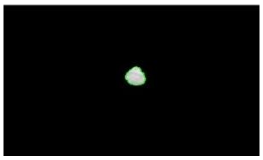

B

Fig. 4The region of Interest, A: Select block from the prostate region, B: Extract a prostate region

3.3 Features Extraction

The methods of feature extraction from the region of interest play very important role in detecting abnormal prostate of CT images. Features of ROI have been proven to be useful in differentiating abnormal and normal prostate.They are first order and second order. In the first order, ROI measures are statistics calculated from an individual pixel and do not consider pixel neighbor relationships. The (Mean intensity, Standard deviation, Root mean square, Kurtosis, Skewness) features are a first-order calculation. In the second order, measures consider the relationship between neighbor relationships.The co-occurrence matrix or co-occurrence distribution is a second order ROI calculation (Contrast, Correlation, Energy, Homogeneity, Entropy and Inverse Difference Moment IDM). The images are classified as normal and abnormal using SVM Classifier. Also, the graph is shown in Figure (5) represents the statistical feature values for the normal and abnormal prostates. The normalized ROI features are evaluated and compared between normal and abnormal groups using independent-samples student’s T-test. If the P value is large than 0.05, it indicates no difference of the feature between two groups is statistically non - significant such as (IDM, Energy, Entropy , Kurtosis). If the P value is less than 0.05, it indicates the difference of the feature between two groups is statistically significant such as (variance , correlation , contrast , Homogeneity, mean, standard deviation , smoothness , Root mean square , Skewness) [11].

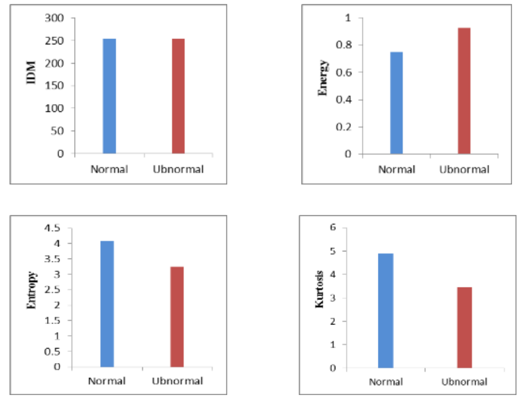

P - value is large than 0.05 indicator non – significant difference between normal and abnormal.

Fig. 5-A Represents the statistical feature values for normal and abnormal prostate

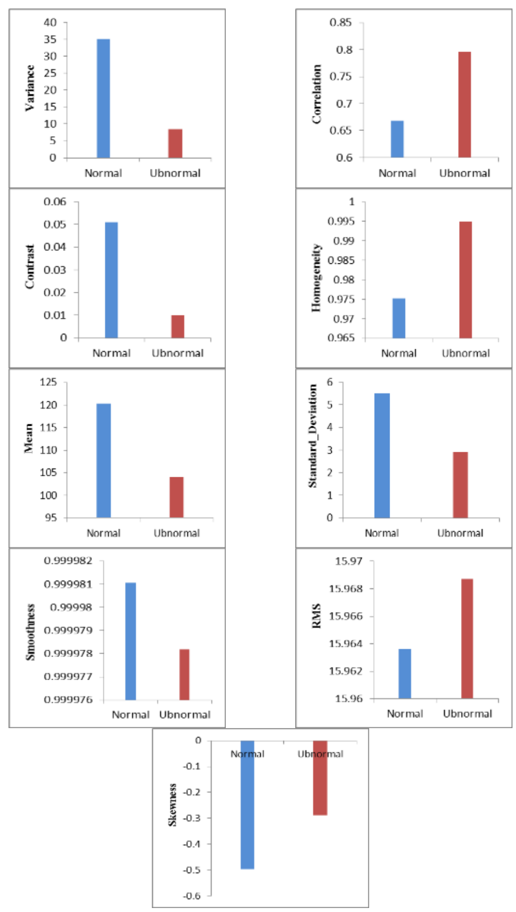

P - value is less than 0.05 indicator significant difference between normal and abnormal.

Fig. 5-B Represents the statistical feature values for normal and abnormal prostate

3.4 Support Vector Machines Classification

Data classification in support vector machines (SVM) classification is the operation that classifies the data into classes. From a training set, techniques in the field can build a forecasting model to classify a new sample that is not in the training set and SVM classification by this method. The training set is given $D = \{(x_i, y_i | i = \overline{1, n}\}$ where x_i is a rows that contains features of images and V. Note that $x_i = (z_1, z_2, z_3, - - - - -)^T$ x_i is a column vector, it means x_i is the samples label whose value is 0 correspond to normal prostate, 1 correspond to abnormal prostate .

The support vector machines classification produce a hyperplane that separates the data into two classes with the maximum distance between the hyperplane and the closest examples (the margin). The hyperplane form is given by:

$$f(w, x) = sign(K(w, x) + b)$$

The hyperplane of the normal vector is w, where K(w, x)=$\Phi(W)^T$ $\Phi(x)$ is the kernel function ϕ is a mathematical function that transforms the data from original space to a feature space, which has higher dimension. The hyperplane separates the feature space into two regions, each class appoint to one region [12].

The second approach of classification for solving the multiclass SVM is the one-against-all (Ovall) approach to classify multiple cases or differentiate between different groups of prostate glands based on the feature extracted from prostate ct images. In Ovall, the multiclass problem is decomposed into m two-class sub-problems.

Let X = $\{x_1, ...x_i ..., x_k\}$ denote the set of k classes. For the k multiclass problem, k two-class classifier models are constructed km = {m1, ... mi, ...mk], where model is trained to separate the class mi (positive class) from the rest classes {X – mi] (negative class) [13].The Implementation SVM classification is shown in figure(6).

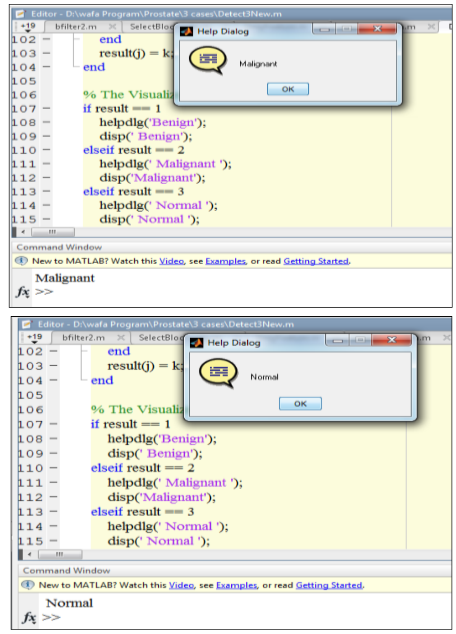

Fig. 6.The application of SVM classification in Matlab R 2015b.

In the first step, 84 samples for training labeled as normal and abnormal groups, and 24 samples for testing. all with 13 statistical features. The program was trained, then for normal and an abnormal condition was tested, The results give 100% accurate. In the second step: 72 training samples labeled to three groups (Normal, benign and malignant) and 36 for testing where each group tested with all of the training data, training, and testing steps are repeated and the performance results are averaged for the estimation of classification rates. The procedure is used to test the SVM with various parameter settings. Performance evaluation is based on the following criteria:

$$Accuracy = \frac{TP + TN}{TP + TN + FP + FN} \times 100$$

where TP (True Positive) and FP (False Positive) are the Number of normal regions classified as normal and abnormal respectively.while TN (True Negative) and FN (False Negative) are the Number of abnormal regions classified abnormal And normal respectively [14], the result are shown in table (1).

Table 1: Accuracy results for SVM and multiclass SVM

SVM performance evaluation (Accuracy)			
Normal & Abnormal test		Normal, Benign and malignant test	
Normal	100%	Normal	92.6%
Abnormal	100%	Benign	75.6%
		Malignant	65.8%

3.5 Prostate Size Measurement

Four samples of the normal prostate of different ages were analyzed for the accuracy of volume estimation using two way :

the first by the ellipsoid model (equation .1) where the prostate volume calculated by measuring the greatest three dimensions of the prostate on CT manually and these measurements were used to determine the volume estimate of the prostate [15,16].

$$V(mm3)= (H \ X \ W \ X \ L \ X \ \pi/6) \qquad (1)$$

Where, (H) is superoinferior dimension; W, anteroposterior dimension; and L, right-left dimension, the dimensions take from singofast view software with a 3D view of the image as shown in figure (7), table (2) show the ellipsoid method for 4 samples.

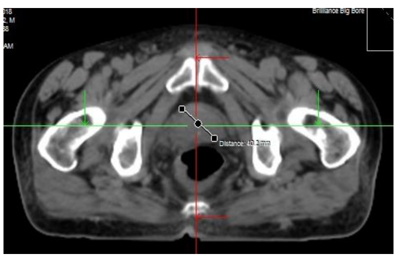

Fig. 7 Measure distance from the 3D view of CT image.

Table 2: Prostate volume of a normal person with different ages using ellipsoid model.

NO.	Age	L (mm)	W(mm)	H(mm)	Volume (cm^3)
1	30	30	32	35	17.6
2	38	33	32	36	19.3
3	44	36	36	39	26.5
4	49	37	35	41	27.8

the second method used frustum model [17] between two consecutive slices with area A_i, A_{i+1} and slice thickness h (equation .2) ,an analysis was made to separate the shape of glands from each slice to obtain the desired images and calculate the area in (pixel) from binary image then convert the area to actual size in mm^2 using equation 3 , finally formula(2) of frustum model applied to determine prostate volume .

$$V(mm^3) = \sum \frac{h}{3} \left(A_i + A_{i+1} + \sqrt{A_i * A_{i+1}} \right) \qquad (2)$$

$$Ai(mm\ 2) = Ai\ (pixel)\ x\ (\ FOV/\ matrix\ size)2 \qquad (\ 3)$$

Where FOV is the field of view (different in each sample, ranging between 380-700),

matrix size = 512 x 512 for all samples.

Studies have shown that the size of the normal prostate gland dimensions has approximately 3 × 3 × 5 cm or a volume of 25 ml. [18]. Sample of prostate volume calculated using frustum model shown in table (3).

Table 3: Prostate volume measurement using frustum model.

Slice NO.	Select ROI from Enhance image	ROI	Area (mm^2)	Volume (cm^3)
86	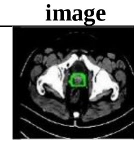		1351.8	
87	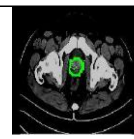	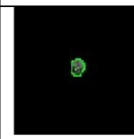	1353.4	
88	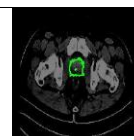	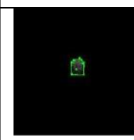	1568.1	27.7
89	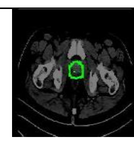	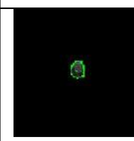	1387.6	
90	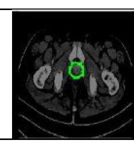	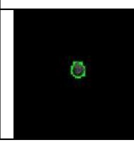	1173.9	

The result of prostate volume measurement by ellipsoid and frustum models for each sample is presented in Table 4. From the table, it is shown that the calculated volume for Iraqi adult normal population ranges from (18.4 cm^3) to (27.8 cm^3) with the mean prostate volume of (23.1 cm^3). This normal volume is acceptable since it is very close to the average prostate volume of an adult.

Table 4: Prostate volume of four samples calculated using two approaches

Sample No.	age	volume (Ellipsoid model) cm^3	volume (Frustum model) cm^3
1	30	17.6	18.4
2	38	19.3	21.5
3	44	26.5	27.6
4	49	27.8	27.7

4. Conclusion

In this work, SVM based pattern recognition methods are demonstrated to identify the classification of normal or abnormal prostate in adult Iraqi male using abdomen CT test , the result showed that the method was successful with 100% accuracy to identify normal and abnormal prostate lesion ,but the accuracy of determining whether the enlargement of prostate is benign or malignant fell to 75% for benign and 65% for malignant, From this, it becomes clear that the CT scan examination is not useful for early identify prostate cancer unless the disease reached advanced stages.

In the second part of work, the size of the prostate calculated in normal adults, using two methods, the prostate size varies with age, where it can become significantly larger in older men. The prostate gland tends to enlarge, around the age of 40. The two methods gave success in the computation of size using the images of CT scan, where they showed a significant match in the results, but the ellipsoid method is faster than frustum method.

References

[1] The Prostate Cancer Research Foundation of Canada. Ending the Threat of Prostate Cancer: Progress Report on Prostate Cancer Research.Toronto, Nov. 2002. Available at: http://www. prostatecancer.ca.

[2] Ganesh Balasubramaniam, Sanjay Talole, Umesh Mahantshetty, Sushama Saoba, Shyam Shrivastava. Prostate Cancer: A Hospital-Based Survival Study from Mumbai, India. Asian Pacific Journal of Cancer Prevention. Vol 14, p. 2595 -2598; 2013

[3] Manju B , K.Meenakshy, R. Gopikakumari," Prostate Disease Diagnosis from CT images using GA optimized SMRT based Texture Features"; International Conference on Information and Communication Technologies (ICICT 2014); 2015, 46; 1692 – 1699; doi: 10.1016/j.procs.2015.02.111; Procedia Computer Science.

[4] S. S. Mohamed, A. M. Youssef, E. F. El-Saadany, and M. M. A. Salama, "Artificial life feature selection techniques for prostate cancer diagnosis using TRUS images". New York: Springer, 2005, Lecture Notes in Computer Science, p. 903–913.

[5] Mark A. Sheppard and Liwen Shih. "Image Texture Clustering for Prostate Ultrasound Diagnosis". In Proceedings of IEEE Ultrasonics Symposium 2007, p. 2473-2476, 2007.

[6] Yinghuan Shi, Shu Liao, Yaozong Gao, Daoqiang Zhang, Yang Gao, and Dinggang Shen. "Prostate Segmentation in CT Images vi a Spatia l- Constrained Transductive Lasso. I EEE Conference on Computer Vision and Pattern Recognition, 2013, pp. 2225-2234,.

[7] M.Petrou and P.G. Sevilla, "I image Processing Dealing with Texture", Wiley Publishers, p. 1-6, 2006.

[8] Zhiwu Liao,Shaoxiang Hu,Zhiqiang Yu,Dan Sun.Medical Image Blind Denoising Using Context Bilteteral Filter. International Conference of Medical Image Analysis and Clinical Application, 2010:12-17.

[9] C.Tomasi, R. Manduchi. Bilateral Filtering for Gray and Color images. Procedings of IEEE international Conference on Computer Vision, Bombay, India, 1998: 839-846.

[10] S. Thurnhofe r and S. K. Mitra, "A general framework for quadratic Volter rafiltersfor edge

[11] enhancement," IEEE Transactions on Image Processing, Jun. 1996,vol. 5, no. 6, p. 950-963,

[12] Anuradha.K , Dr. K. Sankaranarayanan ," Statistical Feature Extraction To Classify Oral Cancers", Journal of Global Research in Computer Science, February 2013,Vo. 4(2).

[13] apnik V, Guyon I, Boser BE. A Training Algorithm for Optimal Margin Classifiers. The 5 Annual Workshop on Computational Learning Theory. Pittsburgh: ACM Press; 1992. p. 144-52.

[14] Dheeb A., Shahnorbanun S., Azizi A., Mohammed A. and Afzan A.," A Hierarchical Classifier For Multiclass Prostate Histopathology Image Gleason Grading", Journal of ICT, 2018, Vol 18, No. 2 , pp: 323–346.

[15] Metehan M., "Support Vector Machine Approach for Classification of Cancerous Prostate Regions", International Journal of Medical and Health Sciences , 2007 ,Vol 1, No 7.

[16] Ng Kent H., Muhammad A.A., Maheza I. Mohamad S.,Heamn N. A., Eko S., " Prostate Volume Measurement Using Transabdominal Ultrasound Scanning", Advances in Environment, Biotechnology and Biomedicine, September 2012, 20-22.

[17] Ng K. H., Muhammad A. A., Maheza I. M., Christina P., Heamn N.A., Eko S., "Prostate Volume Ultrasonography: The Relationship of Body Weight, Height, Body Mass Index and Ethnicity in Transabdominal Measurement" International Journal of Biology and Biomedical Engineering, 2012, Vol 6, Issue 4.

[18] Shally HR and Chitharanjan K," Tumor Volume Calculation Of Brain From Mri Slices", International Journal of Computer Science & Engineering Technology (IJCSET), 2013, Vol. 4, No. 08, p.1126-1132.

[19] Michael M., Wolfgang H., Friedrich A., Germar M. P., Ilona S., Peter R. and Ferdinand F., "Ultrasound of the prostate", International Cancer Imaging Society, 2010, Vol. 10, p.40_48.